

4th International Conference on Advances in Energy Research 2013, ICAER 2013

## Synthesis and characterization of spray deposited Nickel-Zinc ferrite thin films

S. S. Kumbhar<sup>a</sup>, M. A. Mahadik<sup>a</sup>, V. S. Mohite<sup>a</sup>, K. Y. Rajpure<sup>a</sup>, C. H. Bhosale<sup>a</sup> \*

<sup>a</sup>*Electrochemical Materials Laboratory, Department of physics, Shivaji University, Kolhapur 416004, India*

### Abstract

Thin films of nickel-zinc ferrite with general formula  $\text{Ni}_x\text{Zn}_{1-x}\text{Fe}_2\text{O}_4$  (where  $x = 0.5, 0.6, 0.7, 0.8, 0.9, 1.0$ ) has been prepared using spray pyrolysis technique onto the glass substrates at optimized substrate temperature of  $400^\circ\text{C}$ . The nickel nitrate, zinc acetate and ferric nitrate were used as precursor materials with double distilled water as solvent. As deposited films are annealed at  $600^\circ\text{C}$  for 2 hrs. The X-ray diffraction (XRD) analysis reveals that the  $\text{Ni}_x\text{Zn}_{1-x}\text{Fe}_2\text{O}_4$  thin films are polycrystalline with spinel cubic structure. The SEM images shows the films are smooth and uniform in nature. To understand the semiconducting behavior the DC resistivity of films was measured using two point probe method. To know the conduction mechanism of ferrites the AC conductivity of thin films was measured. The linear nature of the graph shows the small type of polarons. Frequency dependence of dielectric constant shows dielectric dispersion due to the Maxwell-Wagner type of interfacial polarization. Impedance spectroscopy used to study electrical behavior of grain or grain boundaries.

© 2014 C.H. Bhosale. Published by Elsevier Ltd. This is an open access article under the CC BY-NC-ND license (<http://creativecommons.org/licenses/by-nc-nd/3.0/>).

Selection and peer-review under responsibility of Organizing Committee of ICAER 2013

**Keywords:** Ni-Zn ferrite thin films; Structural; Morphological; Electrical; Dielectrical properties.

### 1. Introduction

In recent years, the soft magnetic materials have more demands in information and communication technology, because of their high frequency applications [1]. The trend for downsizing electronic equipment's and the potential applications of soft ferrite materials, have lead to the fabrication of thin films of ferrites [2]. Also the thin films of ferrite are used as microwave magnetic devices such as insulators, gyrators, circulators etc.[3].

The bulk component of ferrites cannot be compatible with rapid development of electronic applications but the thin films of ferrite are used in microwave integrated circuits, are expected to replace the surface mounted devices

\* Corresponding author. Tel.: 91-231-2609435; Fax: +91-231-2691533.

E-mail address: [chb\\_phy@unishivaji.ac.in](mailto:chb_phy@unishivaji.ac.in)

(SMD) in near future [4]. The addition of  $\text{Ni}^{2+}$  content in  $\text{ZnFe}_2\text{O}_4$  due to the increasing trend of resistivity and because of their high resistivity, high curie temperature, strong mechanical hardness, excellent soft magnetic properties at high frequency and chemical stability the nickel–zinc ferrites have been widely used as high-performance microwave devices [5]. Nickel-Zinc ferrite used in a electronic devices like TV sets, transformer, microwaves integrated non-reciprocal circuits, memory core devices, radio frequency coil, rod antennas, read–write heads for high-speed digital tape or disk recording. The nickel–zinc ferrites are used for the catalysis applications [6]. Therefore, many kinds of techniques such as chemical vapor deposition (CVD) [7], pulsed laser deposition [8], rf-sputtering [9], sol-gel [10] etc. has been attempted for ferrite film deposition. Among these, spray pyrolysis is one of the most widely used methods because of spray pyrolysis has several advantages such as high purity, excellent control of chemical uniformity, and stoichiometry in multi-component system in comparison with other chemical deposition techniques. The other advantage of the spray pyrolysis method is that it can be adapted easily for production of large-area films [11]. In present work  $\text{Ni}_x\text{Zn}_{1-x}\text{Fe}_2\text{O}_4$  (where  $x = 0.5, 0.6, 0.7, 0.8, 0.9, 1.0$ ) thin films prepared by spray pyrolysis technique. The prepared films are characterized by XRD, SEM, AC conductivity, electrical resistivity, dielectrical properties, and impedance spectroscopy to understand the influence of Ni content in ferrite.

## 2. Experimental

The thin films of  $\text{Ni}_x\text{Zn}_{1-x}\text{Fe}_2\text{O}_4$  (where  $x = 0.5, 0.6, 0.7, 0.8, 0.8, 0.9, 1.0$ ) were synthesized by spray pyrolysis technique. The nickel nitrate  $(\text{NO}_3)_2 \cdot 6\text{H}_2\text{O}$ , zinc acetate  $(\text{CH}_3\text{CO}_2)_2$  and ferric nitrate  $(\text{NO}_3)_3 \cdot 9\text{H}_2\text{O}$  were used as starting precursor materials for the formation of the  $\text{Ni}_x\text{Zn}_{1-x}\text{Fe}_2\text{O}_4$  ferrite thin films. These precursors were dissolved separately in double distilled water for making solution of 0.1 M concentration. Final solution was prepared by mixing these three solutions (1:1:1) ratio. The resulting 30 cc solution was sprayed onto preheated glass substrates. The soda-lime glass substrates were used for film deposition. These substrates were cleaned with doubly distilled water and furthermore boiled in 1M chromic acid for 1 hr to remove sticky particles of oil, grease and then dried in alcoholic vapours. The good quantity thin films were deposited by optimizing various preparative parameters like substrate temperature  $400^\circ\text{C}$ , solution spray rate (2 ml min<sup>-1</sup>), nozzle to substrate distance (32 cm) was kept constant. The synthesized films are amorphous in nature, hence to enhance the crystallinity, the films were annealed at  $550^\circ\text{C}$  for 2 hrs. The structural properties of  $\text{Ni}_x\text{Zn}_{1-x}\text{Fe}_2\text{O}_4$  ferrite (with  $x = 0.5, 0.6, 0.7, 0.8, 0.9$ , and  $1.0$ ) thin films were studied by using Bruker D2: PhaserX-ray diffractometer using  $\text{CuK}_\alpha$  radiation. The surface morphology was studied by using a JEOL JSM- 6360 scanning electron microscope (SEM). The dielectric constant ( $\epsilon'$ ), loss tangent ( $\tan\delta$ ) and impedance were measured at room temperature in the frequency range 20 Hz to 1 MHz using LCR Meter Bridge (model HP 4284 A). The resistivity measured by using two probe method.

## 3. Results and discussion

### 3.1 Structural properties

Fig.1. shows the X-ray diffraction pattern of  $\text{Ni}_x\text{Zn}_{1-x}\text{Fe}_2\text{O}_4$  films deposited at  $400^\circ\text{C}$ . As deposited films at substrate temperature  $400^\circ\text{C}$  are amorphous in nature, hence these films are annealed at  $550^\circ\text{C}$ . These annealed  $\text{Ni}_x\text{Zn}_{1-x}\text{Fe}_2\text{O}_4$  thin films are polycrystalline in nature and having orientation along (311) plane. The matching of observed and standard 'd' values have been made using JCPDS card No.08-0234 which confirms the spinel cubic structure. The other planes such as (220), (400), (422), (511) and (440) are also observed with smaller intensity. X-ray diffraction patterns shows the intensity of diffracted plane is increases when  $x = 1.0$  and the peaks are slightly shifted which may be due to the influence of nickel content. As Ni content increases then lattice parameter decreases from 7.1 to 7.0. The average crystallite size 'D' was calculated by using Scherrer's formula,

$$D = (0.9 \times \lambda) / (\beta \times \cos \theta) \quad (1)$$

where,  $\lambda$  the wavelength of X-rays ( $1.5406 \text{ \AA}$ ),  $\beta$  is the full-width at half-maximum in radian, and  $\theta$  the angle of diffraction. It is seen that as the nickel content increases the crystallite size varies from 20 to 36 nm.

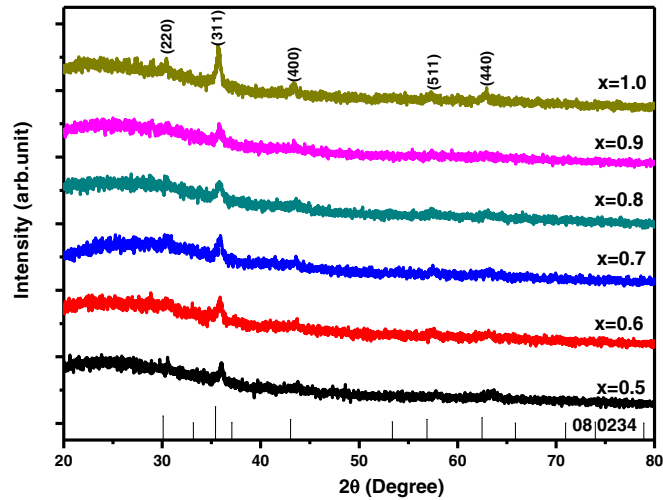


Fig.1. X-ray diffraction pattern of  $\text{Ni}_x\text{Zn}_{1-x}\text{Fe}_2\text{O}_4$  thin films, from  $x=0.5$  to  $x=1.0$

### 3.2 Morphological properties

The surface morphology of the annealed  $\text{Ni}_x\text{Zn}_{1-x}\text{Fe}_2\text{O}_4$  thin films deposited on to glass substrate is shown in fig.2. From these SEM images it is observed that, the surface of the film are smooth and having uniform nature. Some overgrowth on the surface of the film can be seen.

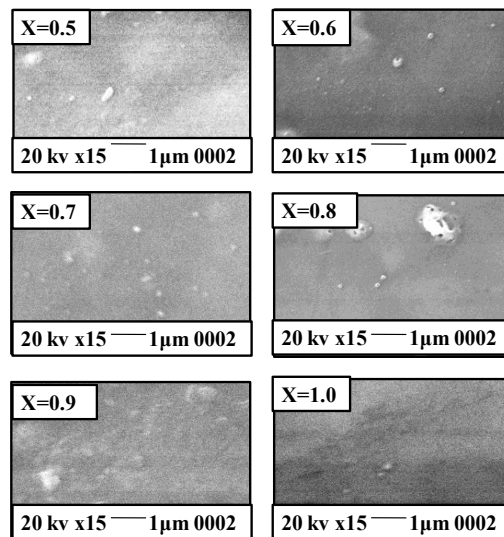


Fig.2. Scanning electron micrographs of  $\text{Ni}_x\text{Zn}_{1-x}\text{Fe}_2\text{O}_4$  thin films, from  $x = 0.5$  to  $x = 1.0$

### 3.3 Electrical properties

The variation of DC resistivity of  $\text{Ni}_x\text{Zn}_{1-x}\text{Fe}_2\text{O}_4$  thin films (where  $x = 0.5, 0.6, 0.7, 0.8, 0.9, 1.0$ ) with temperature is shown in fig.3. It is observed that the resistivity ( $\rho$ ) of thin films decrease with increasing temperature due to the semiconducting nature of the samples and the increase in the thermally activated drift mobility of charge carriers according to the hopping conduction mechanism [12]. In ferrites, the electrons are localized and there is a little overlap between the wave functions of ions situated on adjacent sites. In the presence of lattice vibrations, the

ions occasionally coming so close then the probability of transfer of electron from one ion to another is very high. Hence the mobility is temperature dependent and is characterized by activation energy [13]. The activation energy is calculated by using formula,

$$\rho = \rho_0 \exp\left(\frac{\Delta E}{kT}\right) \quad (2)$$

where, ' $\Delta E$ ' is the activation energy,  $\rho$  the resistivity at room temperature, ' $k$ ' the Boltzmann constant and ' $\rho_0$ ' is the temperature independent constant.

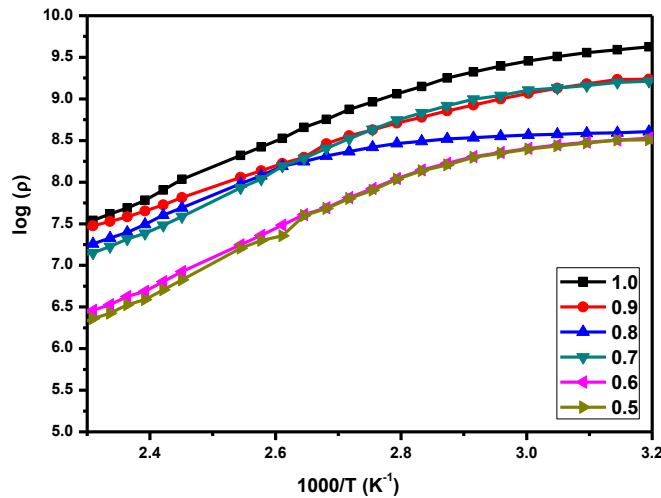


Fig.3. Resistivity measurement of  $\text{Ni}_x\text{Zn}_{1-x}\text{Fe}_2\text{O}_4$  ferrite thin films for  $x = 0.5$  to  $x = 1.0$

In order to understand the conduction mechanism of ferrites the conductivity can be studied. Figure 4 shows the graph of AC conductivity as a function of applied frequency at room temperature of  $\text{Ni}_x\text{Zn}_{1-x}\text{Fe}_2\text{O}_4$  ferrite thin films (with  $x = 0.5, 0.6, 0.7, 0.8, 0.9, 1.0$ ). In present case, conductivity increases with increasing applied frequency. This is due to the as frequency of the applied field increases, hopping of charge carriers also increases thereby the conductivity. The conductivity of the samples was calculated from the dielectric parameters using the relation

$$\sigma_{ac} = \varepsilon' \varepsilon_0 \omega \tan \delta \quad (3)$$

where,  $\varepsilon'$  is dielectric constant,  $\varepsilon_0$  permittivity of free space, ' $\omega$ ' the angular frequency,  $\tan \delta$  is the loss tangent. Fig. 4. shows that the conductivity is increases with increase in frequency for all the compositions under study. Linear variation of AC conductivity indicates that the conduction occurs by hopping of charge carriers among localized states.

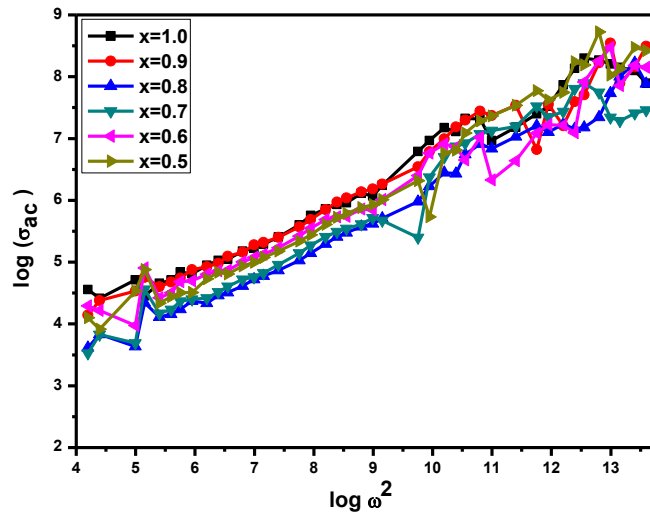


Fig.4. Variation of AC conductivity with frequency at room temperature for  $\text{Ni}_x\text{Zn}_{1-x}\text{Fe}_2\text{O}_4$  thin films

### 3.4 Dielectric properties

Fig.5. shows the variation of dielectric constant with frequency at room temperature. The dielectric properties of thin films are affected by many factors, compositional inhomogeneties, grain size, defect chemistry, oxygen vacancies, strain and stress, and dopants [14]. It has been seen that the dielectric constant decreases with increasing frequency. These monotonically decreasing value of dielectric constant on increasing frequency may be attributed to a combined contribution due to electronic, ionic, and interfacial polarization at low frequencies [15]. The large value of dielectric constant at lower frequencies is attributed to different types of polarizations (electronic, atomic, ionic, interfacial etc). The polarization at lower frequencies may result from the hopping mechanism of  $\text{Fe}^{2+}/\text{Fe}^{3+}$  ions [16].

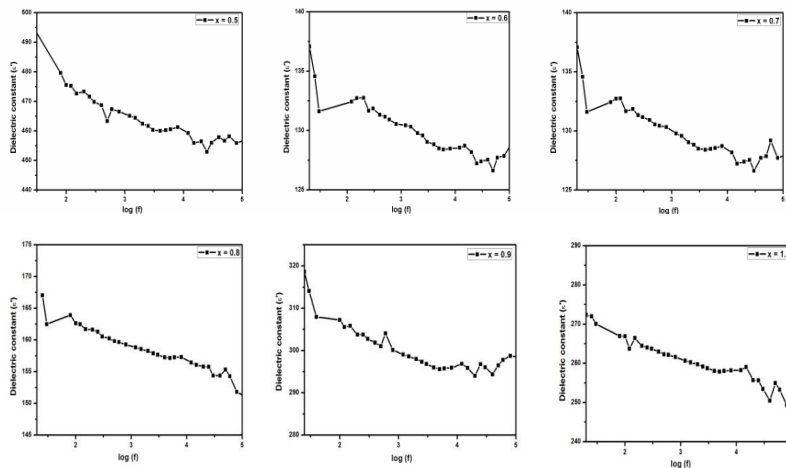


Fig.5. Variation of Dielectric constant with frequency at room temperature for  $\text{Ni}_x\text{Zn}_{1-x}\text{Fe}_2\text{O}_4$  thin films

Fig.6. shows the variation of dielectric loss tangent ( $\tan\delta$ ) of  $\text{Ni}_x\text{Zn}_{1-x}\text{Fe}_2\text{O}_4$  ferrite thin films in the

frequency range 20Hz – 1MHz. It is due to similar behavior like dielectric constant on the basis of koop's phenomenological theory [17].

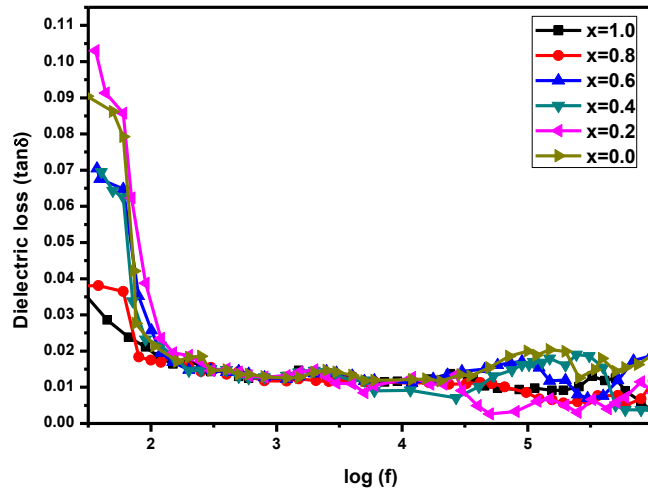


Fig. 6. Variation of dielectric loss with frequency at room temperature for  $\text{Ni}_x\text{Zn}_{1-x}\text{Fe}_2\text{O}_4$  thin films.

### 3.5 Impedance spectroscopy

Fig.7. shows the impedance spectra of  $\text{Ni}_x\text{Zn}_{1-x}\text{Fe}_2\text{O}_4$  ferrite thin films deposited at 400 °C substrate temperatures. The impedance spectrum is also called Nyquist plot or coal-coal plot. Impedance spectrum is the plot of the imaginary ( $Z''$ ) versus real ( $Z'$ ) part of the impedance. Usually there are two semicircular arcs, grains and grain boundaries.

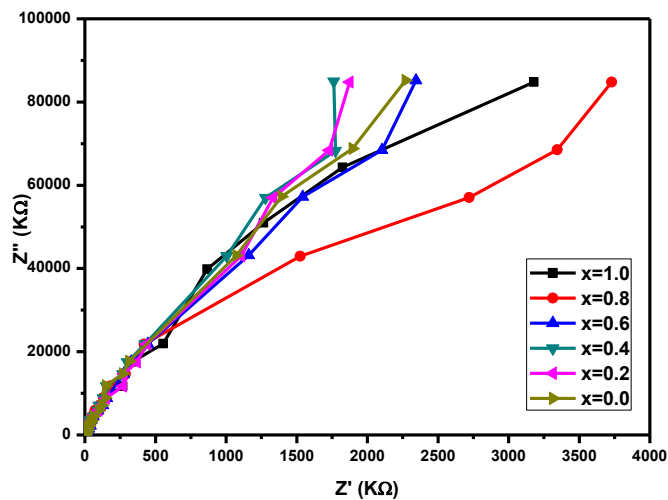


Fig.7. Complex impedance spectra for  $\text{Ni}_x\text{Zn}_{1-x}\text{Fe}_2\text{O}_4$  thin films from  $x=0.5$  to  $x=1.0$

In the present study, only single semicircular arcs have been observed. These single semicircle of thin film is not fully displayed, the diameter may be extrapolated readily which indicates that the impedance mainly

originates from the contribution of the grain interior because the grain boundary usually exhibits a much higher resistance than that of the grain interior because of the potential barrier in grain boundary [18].

#### 4. Conclusions

Preparation of  $\text{Ni}_x\text{Zn}_{1-x}\text{Fe}_2\text{O}_4$  (with  $x = 0.5, 0.6, 0.7, 0.8, 0.9, 1.0$ ) by using spray pyrolysis technique is possible. The XRD result confirms the purity of the phase with peak orientation along (311) confirms the formation of spinel ferrite. The SEM images show the surfaces of the films are smooth and uniform in nature. The increase in the Ni content in the  $\text{ZnFe}_2\text{O}_4$  the resistivity of films samples increases. The conduction mechanism can be understood from the AC conductivity studies. The dielectric constant decreases with increases increase in frequency of applied field. The grain boundary behaviour can be studied from the impedance spectroscopy.

#### Acknowledgements

S. S. Kumbhar is thankful to the Department of Physics, Shivaji University Kolhapur for awarding the Departmental Research Fellowship (DRF) for financial support.

#### References

- [1] Yanagihara M, Kawano K, Honda T, Kyomen T, Hanaya M. Formation of Ni-Zn ferrite nano-crystalline thin films by rf magnetron sputtering with changing substrate temperatures. *Thermochim. Acta* 2012; 532; 145-147.
- [2] Li L, Peng L, Li Y, Zhu X. Structure and magnetic properties of Co-substituted Ni Zn ferrite thin films synthesized by the sol-gel process. *J. Mag. Mag. Materials* 2012; 324; 60-62.
- [3] Gupta N, Verma A, Kashyap SC, Dube DC. Dielectric behavior of spin-deposited nanocrystalline nickel-zinc ferrite thin films processed by citrate-route. *Solid.State.Commu* 2005; 134; 689-69.
- [4] Sun K, Lan Z, Yu Z, Nie X. Characterization and magnetic properties of polyethylene glycol modified NiZn ferrite thin films. *Curr. App. Physics* 2011; 11; 472-475.
- [5] Zi Z, Lei H, Zhu X, Wang B, Zhang S, Zhu X, Song W, Sun Y. Influence of annealing temperature on surface morphology and magnetic properties of  $\text{Ni}_{0.7}\text{Zn}_{0.3}\text{Fe}_2\text{O}_4$  ferrite thin films. *Mater. Sci. Engin. B* 2010; 167; 70-73.
- [6] Saba AE, Elsayed EM, Moharam MM, Rashad MM, AboShahba RM. Structure and magnetic properties of  $\text{Ni}_x\text{Zn}_{1-x}\text{Fe}_2\text{O}_4$  thin films prepared through electrodeposition method. *J. Mater. Sci.* 2011; 46; 3574-3582.
- [7] Lane PA, Wright PJ, Crosbie MJ, Pitt AD, Reeves CL, Cockayne B, Jones AC, Leedham TJ. Liquid injection metal organic chemical vapour deposition of nickel zinc ferrite thin films. *J. Cry. Growth* 1998; 192; 423-429.
- [8] Misu T., Sakamoto N., Shinozaki K., Adachi N., Suzuki H., Wakiya N., Magnetic and optical properties of  $\text{MgAl}_2\text{O}_4\text{-(Ni}_{0.5}\text{Zn}_{0.5})\text{Fe}_2\text{O}_4$  thin films prepared by pulsed laser deposition. *Sci. Technol. Adv. Mater.* 2011; 12; 034-408.
- [9] Hellicar NJ, Young A, Biggers JV. Preparation and Characteristics of Thin Films of Nickel Zinc Ferrite. *J. Vac. Sci. Technol.* 1969; 6; 676.
- [10] Sedlar M, Matejec V, Grygar T, Kadlecova J. Sol-gel processing and magnetic properties of nickel zinc ferrite thick films. *Ceram. International* 2000; 26; 507-512.
- [11] Shinde SS, Bhosale CH, Rajpure KY. Structural, optical, electrical and thermal properties of zinc oxide thin films by chemical spray pyrolysis. *J. Mole. Structure.* 2012; 1021; 123-129.
- [12] Patil DR, Chougule SS, Lokare SA, Chougule BK. Electrical properties of  $x\text{NiFe}_2\text{O}_4 + (1-x)\text{Ba}_{0.7}\text{Sr}_{0.3}\text{TiO}_3$  composites. *J. Allo. Compounds* 2008; 452; 414-418.
- [13] Kambale RC, Adhate NR, Chougule BK, Kolekar YD. Magnetic and dielectric properties of mixed spinel Ni-Zn ferrites synthesized by citrate-nitrate combustion method. *J. Allo.compounds*, 491 (2010) 372-377.
- [14] James AR. Strain effects on the dielectric properties of epitaxial  $\text{SrTiO}_3$  thin films grown by pulsed laser deposition. *Ferroelectrics*.2005; 327:121-126.
- [15] Zhaouadi H, Ghodbane O, Hosni F, Touati F. *Interna. Scho.Rese.Network. ISRN Spectroscopy*; volume 2012; 2012:1-8.
- [16] Mallapur MM, Shaikh PA, Kambale RC, Jamadar HV, Mahamuni PU, Chougule BK. *J. Allo. Compounds* 2009; 479:797-802.
- [17] Patil DR, Chougule BK. *Mater. Chem. Physics* 2009; 117:35-40.
- [18] Wu J, Wang Xiao JD, Zhu J. Impedance spectroscopy of bilayered bismuth ferrite thin films. *J. Appl. Physics.* 2011; 110; 064104.